Article

Influence of Temperature and Concentration on the Self-Assembly of Nonionic C_iE_j Surfactants: A Light Scattering Study

Peter Kroll, Julius Benke, Sabine Enders, Christoph Brandenbusch,* and Gabriele Sadowski*

Read Online

ACCESS | Metrics & More | Article Recommendations | Supporting Information

ABSTRACT: Nonionic poly(ethylene oxide) alkyl ether (C_iE_j) surfactants self-assemble into aggregates of various sizes and shapes above their critical micelle concentration (CMC). Knowledge on solution attributes such as CMC as well as aggregate characteristics is crucial to choose the appropriate surfactant for a given application, e.g., as a micellar solvent system. In this work, we used static and dynamic light scattering to measure the CMC, aggregation number (N_{agg}), and hydrodynamic radius (R_h) of four different C_iE_j surfactants (C_8E_5, C_8E_6, $C_{10}E_6$, and $C_{10}E_8$). We examined the influence of temperature, concentration, and molecular structure on the self-assembly in the vicinity of the CMC. A minimum in the CMC vs temperature curve was identified for all surfactants investigated. Further, extending the hydrophilic and hydrophobic chain lengths leads to an increase and decrease of the CMC, respectively. The size of the aggregates strongly depends on temperature. N_{agg} and R_h increase with increasing temperature for all surfactants investigated. Additionally, N_{agg} and R_h both increase with increasing surfactant concentration. The data obtained in this work further improve the understanding of the influence of temperature and molecular structure on the self-assembly of C_iE_j surfactants and will further foster their use in micellar solvent systems.
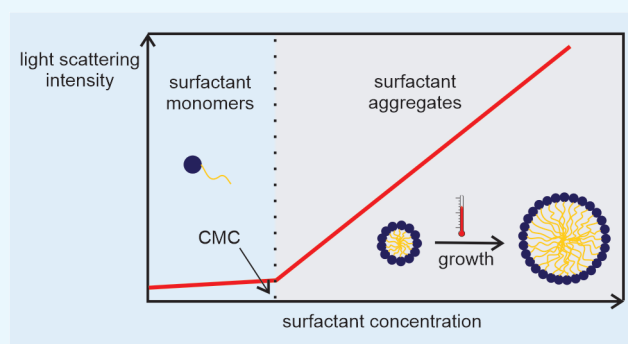
1. INTRODUCTION

Surfactants are amphiphilic molecules possessing a hydrophilic head and a hydrophobic tail group. Due to their amphiphilic nature, they self-assemble into aggregates (e.g., micelles, vesicles) in a given solvent above their critical micelle concentration (CMC). These aggregates can solubilize otherwise insoluble compounds, making them suitable for many industrial applications. Surfactant aggregates are used in pharmaceutical formulations to solubilize poorly water-soluble drugs and thus to enhance the bioavailability of these drugs.[1,2] In enhanced oil recovery, in food products, and in cosmetics, surfactants are used to produce (micro)emulsions by drastically reducing the interfacial tension between immiscible liquids.[3−5]

In recent years, so-called micellar solvent systems have gained increasing attention when used as "green" reaction media in the chemical and biochemical industry.[6−9] There, especially nonionic poly(ethylene oxide) alkyl ether surfactants are of interest.[10] These surfactants consist of an alkyl chain as hydrophobic tail and an ethylene oxide chain as hydrophilic head. They are thus denoted as C_iE_j, where i is the number of C atoms in the alkyl chain and j is the number of ethylene oxide units in the ethylene oxide chain.

Although C_iE_j surfactants were studied extensively in the last decades,[11] experimental data available in the open literature display a striking degree of variation as pointed out in a recent review by Swope et al.[12] Even for the most basic properties of surfactant solutions, such as the CMC and the aggregation number (N_{agg}), values reported in the literature differ significantly.[12,13] Possible reasons for this were elucidated extensively in the work of Swope et al.[12] One straightforward reason is the application of different measurement techniques with different sensitivities for the respective measures. For example, static light scattering (SLS) and dynamic light scattering (DLS) are often used to measure N_{agg}. However, only SLS gives a direct measurement of N_{agg} via the mass-averaged molecular weight (M_W) of the aggregates. DLS measures the translational diffusion coefficient (D_t), which can be used to compute a hydrodynamic radius (R_h) of the aggregates. Assumptions about the shape and hydration of the aggregates are thus necessary to calculate N_{agg} from DLS measurements. Consequently, DLS-derived values of N_{agg} should be used with caution.

Table 1. CMCs for All Investigated Surfactants of This Work[a]

	C_8E_5		C_8E_6		$C_{10}E_6$		$C_{10}E_8$	
				CMC				
$T/°C$	/g L^{-1}	/10^3 mol L^{-1}	/g L^{-1}	/10^3 mol L^{-1}	/g L^{-1}	/10^3 mol L^{-1}	/g L^{-1}	/10^3 mol L^{-1}
15	4.49	12.81	5.34	13.54	0.43	1.02	0.75	1.47
25	3.37 (0.01)	9.61 (0.03)	3.91 (0.07)	9.91 (0.18)	0.35 (0.00)	0.83 (0.01)	0.56 (0.01)	1.10 (0.02)
30	3.24	9.24	3.64	9.93	0.33	0.78	0.52	1.02
40	2.87	8.12	2.91	7.38	0.27	0.64	0.40	0.78
50	2.61	7.45	2.63	6.67	0.28	0.66	0.37	0.72
55	2.68	7.65			0.29	0.67		
60			2.75	6.97			0.36	0.70

[a]Temperatures between 15 and 60 °C were studied. For C_8E_5 and $C_{10}E_6$, the highest temperature investigated was 55 °C due to an LLE in water at around 60 °C. Values in parentheses (25 °C) give the standard deviations out of two measurements of independent samples.

Additionally, both SLS and DLS measurements are sensitive toward attractive or repulsive forces between the aggregates.[14] These forces lead to either an increase (attractive forces) or decrease (repulsive forces) of the intensity of the scattered light, with surfactant/aggregate concentrations increasing beyond the CMC. Therefore, light scattering intensities measured at several concentrations are usually extrapolated to infinite dilution to obtain M_W using Zimm's procedure.[15] However, due to the concentration dependence of M_W, an extrapolation to infinite dilution is not possible for surfactant aggregates.[16] Therefore, we studied concentrations in the vicinity of the CMC, where interactions between the aggregates are negligible and M_W can be computed directly from the measured intensity of the scattered light. Moreover, light scattering intensity increases significantly near the binodal curve of a liquid−liquid equilibrium (LLE) due to concentration fluctuations.[17] C_iE_j surfactants exhibit an LLE in water at elevated temperatures. The onset of this LLE at a given concentration is often referred to as cloud point. Light scattering intensities of a surfactant solution measured near the binodal curve (that is the cloud point) of a C_iE_j solution have to be evaluated with caution due to contributions from fluctuations in the vicinity of the LLE to the overall light scattering intensity.

A further aspect is the general behavior of the CMC and N_{agg} of C_iE_j surfactants with increasing temperature, which is controversially disputed in the literature. While some authors report a monotonic decrease of the CMC with increasing temperature,[18,19] others found a minimum in the CMC vs temperature curve at elevated temperatures.[20] Studies that only reveal a monotonic decrease in the CMC often only considered temperatures up to 40 °C. It is thus fair to assume that 40 °C is too low to observe the minimum in the CMC. This is supported by the fact that for C_iE_j surfactants and for p,t-octylphenol poly(ethylene oxide) glycol monoether surfactants (a similar class of nonionic surfactants), the minimum in the CMC vs temperature curve is present at around 50 °C.[20−22]

The same controversial dispute applies to the behavior of N_{agg} for C_iE_j surfactants with increasing temperature.[23] As a matter of fact, the scattering intensity of aqueous C_iE_j solutions (constant surfactant concentration above CMC) increases with increasing temperature. Some authors solely attributed this increase to concentration fluctuations due to the existence of an LLE at elevated temperatures without considering any growth of the surfactant aggregates. However, other groups found that C_iE_j aggregates grow with increasing temperature

and that these fluctuations only start to dominate the scattering intensity when closely approaching the LLE of the solution.[19,24] Thus, to minimize any contributions from fluctuations near the LLE to the measured light scattering intensity and thus to N_{agg} measurements, we only determined N_{agg} for temperatures 10 K below the respective cloud-point temperature (LLE phase boundary) of the solution.

In this work, we studied the influence of temperature, concentration, and molecular structure of the surfactant (hydrophilic and hydrophobic chain lengths) on the CMC, N_{agg}, and R_h values of four different nonionic C_iE_j surfactants, namely, pentaethylene glycol monooctyl ether (C_8E_5), hexaethylene glycol monooctyl ether (C_8E_6), hexaethylene glycol monodecyl ether ($C_{10}E_6$), and octaethylene glycol monodecyl ether ($C_{10}E_8$). We measured the CMC at different temperatures between 15 and 60 °C to identify the minimum in the CMC vs temperature curve using SLS. By varying both the hydrophilic and the hydrophobic chain lengths, the influence of the surfactant's molecular structure on the minimum in the CMC vs temperature curve was elucidated. Further, the influences of temperature and molecular structure of the surfactant on the size (N_{agg}, R_h) of the aggregates were examined using SLS and DLS.

Additionally, growth of the surfactant aggregates with concentration was studied. We investigated concentrations in the vicinity of the CMC so that interactions between the surfactant aggregates were negligible and any increase in the scattered light could be related directly to the growth of the surfactant aggregates. The results presented in this work lead to a deeper understanding of the aggregation behavior of C_iE_j surfactants near the CMC. Detailed knowledge about the influences of temperature, concentration as well as molecular structure on the self-assembly of the investigated surfactants eases the choice of suitable surfactants for a given application and their application in micellar solvent systems.

2. RESULTS

2.1. Critical Micelle Concentration. The CMCs were determined for four nonionic surfactants considered in this work (C_8E_5, C_8E_6, $C_{10}E_6$, and $C_{10}E_8$). CMCs were studied in the temperature range of 15−60 °C to determine the influence of increasing temperature on the CMC. For C_8E_5 and C_8E_6, the highest temperature measured was 55 °C due to a liquid−liquid phase separation in water at higher temperatures. Experiments were carried out using SLS analytics as described in Section 5. Measured SLS intensities for at least 10 surfactant concentrations below and above the CMC were extrapolated
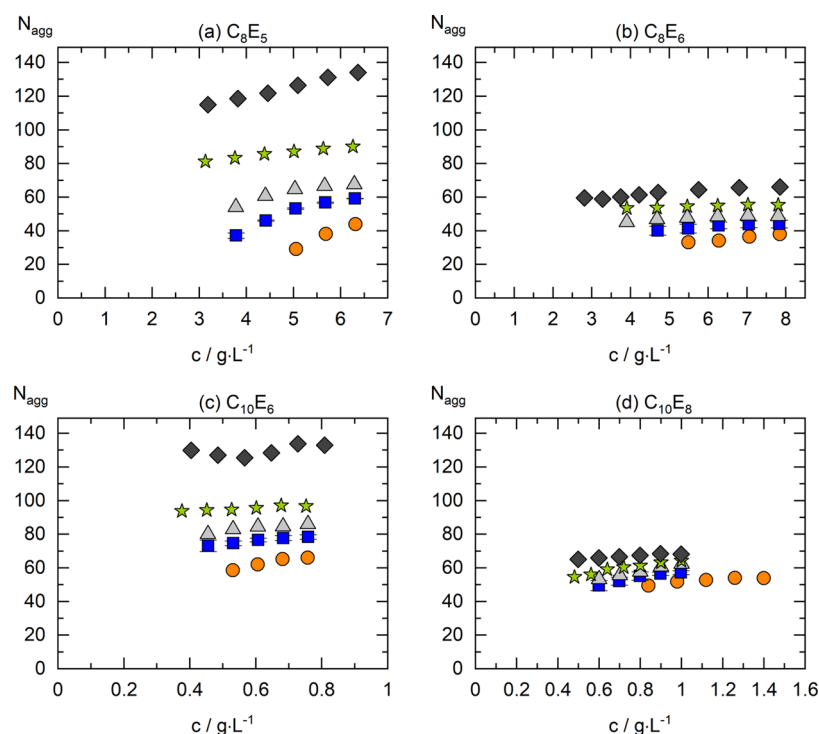
Figure 1. N_{agg} for (a) C_8E_5, (b) C_8E_6, (c) $C_{10}E_6$, and (d) $C_{10}E_8$ at concentrations near the CMC and temperatures from 15 to 50 °C. Temperatures are indicated as follows: circles, 15 °C; squares, 25 °C; triangles, 30 °C; stars, 40 °C; diamonds, 50 °C. Error bars at 25 °C give the standard deviations out of two independent measurements.

linearly, and the CMC was taken as the intersection point. CMCs are listed in Table 1. Measured raw SLS intensities (expressed as $R(\theta)$) for all concentrations and temperatures studied can be found in Figures S1−S4 (Supporting Information).

For all surfactants investigated, CMCs are decreasing monotonically with increasing temperature in the considered temperature range (15−40 °C). The decrease in CMC is more intense at lower temperatures (around 15−25 °C) and levels off at higher temperatures (40−50 °C). However, further increasing the temperature to 50 °C or above does not lead to a decrease of the CMC (e.g., for $C_{10}E_6$) but to a slight increase from 0.27 to 0.28 g L^{-1}. Increasing the temperature to 55 °C amplifies this increase of the CMC. This behavior was also found for C_8E_5, C_8E_6, and $C_{10}E_8$ in the temperature range of 50−60 °C. All investigated surfactants thus show a minimum in their CMC vs temperature curve at around 50 °C.

The results shown in Table 1 further reveal the effect of the ethylene oxide chain length and carbon chain length on the CMC. Increasing the chain length of the hydrophilic ethylene oxide units from E_6 to E_8 at a fixed C_{10} leads to an increase by 74 and 32% in the CMC at 15 and 50 °C, respectively. In contrast, increasing the hydrophobic carbon chain length from C_8 to C_{10} at fixed E_6 leads to a decrease of the CMC by approximately 1 order of magnitude from 3.91 to 0.35 g L^{-1} at 25 °C.

2.2. Aggregation Number. Aggregation numbers were measured for the four nonionic surfactants (C_8E_5, C_8E_6, $C_{10}E_6$, and $C_{10}E_8$) in the temperature range of 15−50 °C to determine the influence of increasing temperature. Furthermore, for all temperature steps considered (15, 25, 30, 40, and 50 °C), N_{agg}'s were also determined at surfactant concentrations ranging from the CMC to approximately 2 times the CMC to elucidate the influence of increasing surfactant

concentrations on N_{agg} at a constant temperature. N_{agg}'s were obtained from SLS measurements as described in Section 5. The refractive index increments dn/dc of the surfactant aggregates that are required to obtain N_{agg} from SLS measurements were measured for all surfactants considered at all temperatures investigated and can be found in Table S1 (Supporting Information). Figure 1 shows the N_{agg} values at different temperatures and concentrations for all surfactants investigated. The raw data from Figure 1 can be found in Tables S2−S5 in the Supporting Information.

For all surfactants investigated, N_{agg} increases with increasing temperature with the magnitude of the increase of N_{agg} differing significantly between the surfactants considered. While N_{agg} of C_8E_5 increases up to 3-fold upon increasing the temperature from 15 to 50 °C, the N_{agg} value of C_8E_6 only increases 1.3-fold within the same temperature interval. Further, the impact of temperature on N_{agg} is more profound at higher temperatures. However, N_{agg} also increases with increasing surfactant concentration. This is especially pronounced for C_8E_5 showing an increase in N_{agg} from 37 to 59 at 25 °C when increasing the surfactant concentration from 3.78 to 6.31 g L^{-1}, respectively. The same behavior is true for N_{agg} of C_8E_6, $C_{10}E_6$, and $C_{10}E_8$ (increases with concentration near the CMC), although the growth for these surfactants is less pronounced compared to C_8E_5.

Besides temperature and concentration, also the molecular structure of the surfactant influences N_{agg}. An extension of the hydrophobic chain length from C_8 to C_{10} at a fixed E_6 leads to an increase in N_{agg}. For example, N_{agg} increases by about 30 and 70 molecules at temperatures of 15 and 50 °C, respectively. In contrast, extending the ethylene oxide chain from E_5 to E_6 and from E_6 to E_8 at fixed C_8 and C_{10}, respectively, leads to a decrease of N_{agg}.
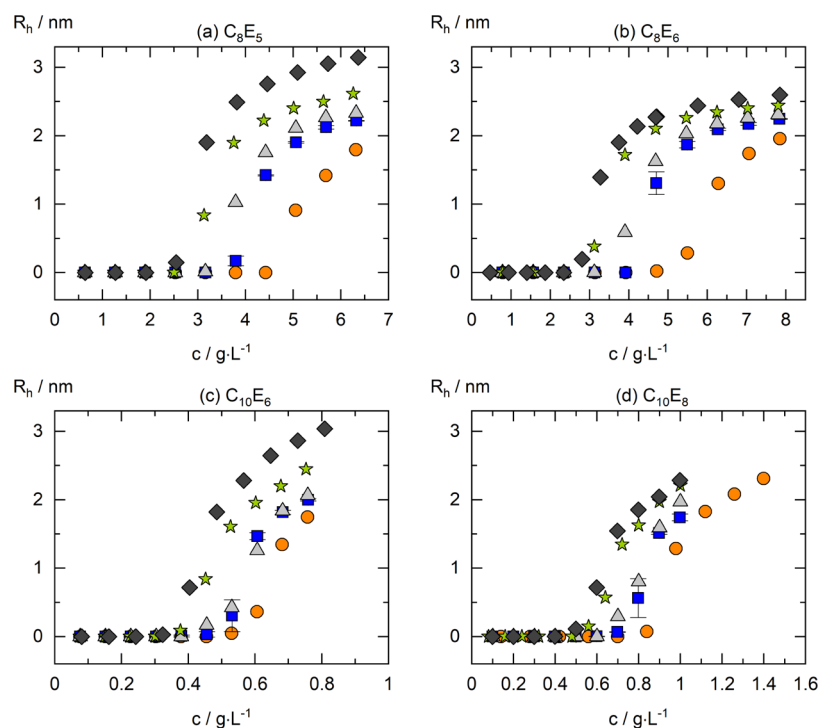
Figure 2. Hydrodynamic radius (R_h) of (a) C_8E_5, (b) C_8E_6, (c) $C_{10}E_6$, and (d) $C_{10}E_8$ at concentrations below and above the CMC. At concentrations below the CMC, no R_h was detectable. Temperatures are indicated as follows: circles, 15 °C; squares, 25 °C; triangles, 30 °C; stars, 40 °C; diamonds, 50 °C. Error bars at 25 °C give the standard deviations obtained from two independent measurements.

2.3. Hydrodynamic Radius. Hydrodynamic radii of all surfactants investigated (C_8E_5, C_8E_6, $C_{10}E_6$, $C_{10}E_8$) were measured in the temperature range of 15−50 °C to elucidate the influence of temperature on R_h. Furthermore, surfactant concentrations ranging from the CMC to 2 times the CMC were investigated at a constant temperature to reveal the influence of increasing concentration on R_h near the CMC. R_h was computed from the translational diffusion coefficient D_t, which was measured via DLS, using the Stokes−Einstein equation as described in Section 5. Figure 2 shows the results for all temperatures and concentrations investigated. The raw data from Figure 2 can be found in Tables S2−S5 in the Supporting Information.

For concentrations below the CMC, no R_h was detectable due to the absence of surfactant aggregates at these concentrations. Exceeding the CMC leads to an abrupt increase in R_h. This increase flattens upon further increasing the surfactant concentration. This is especially pronounced for C_8E_6 but is also present for the other surfactants investigated. However, considering the effect of temperature on R_h, it can be seen that R_h is increasing with increasing temperature, e.g., for C_8E_5, R_h is increasing from 1.78 to 3.15 nm (an increase in R_h of almost 80%) at a fixed surfactant concentration of 6.3 g L^{-1} and temperatures ranging from 15 to 50 °C, respectively. For C_8E_6, this increase in R_h is less pronounced, with R_h increasing only by 30% (from 1.96 to 2.60 nm) at 7.8 g L^{-1} and 15 or 50 °C, respectively.

3. DISCUSSION

3.1. Effect of Temperature and the Molecular Structure of Surfactant on the CMC.
As presented in Section 2.1, the CMCs of all surfactants investigated in this work strongly depend on temperature. For $C_{10}E_6$, the CMC first decreases monotonically in the temperature range of

15−40 °C, before showing a minimum near 50 °C. Such a minimum in the CMC versus temperature curve was also found for C_8E_5, C_8E_6, and $C_{10}E_8$ in this work and is a well-known phenomenon for many ionic and nonionic surfactants.[21,26] As the temperature increases, hydrogen bonding between the ethylene oxide chain and the surrounding water molecules is weakened and dehydration of the ethylene oxide groups occurs.[22] Thus, the surfactant molecule becomes more hydrophobic shifting the onset of micelle formation toward lower concentrations. This effect is known to be stronger for longer ethylene oxide chains[22] and can be confirmed by our data comparing C_8E_5 with C_8E_6 and $C_{10}E_6$ with $C_{10}E_8$ (see Table 1).

Simultaneously with the weakening of the hydrogen bonds for the ethylene oxide chain, the alkyl chain of the surfactant possesses a minimum solubility in water around room temperature.[27,28] Starting from there, the alkyl chain of the surfactant molecules starts to become more soluble with increasing temperature. Hence, the contribution of the hydrophobic alkyl chain is shifting the onset of micelle formation toward higher concentrations with increasing temperature.[29] Therefore, in the low-temperature region (15−40 °C), the contribution of the ethylene oxide chain dominates and the CMC decreases with increasing temperature. At the minimum in the CMC vs temperature curve, the contribution of the hydrophobic alkyl chain starts to predominate and the CMC increases upon further increasing the temperature.[20]

CMC data for the investigated surfactants in the literature comprise a rather broad concentration range as pointed out recently by Swope et al.[12] These authors evaluated CMC data at 25 °C for C_iE_j surfactants available in the literature and found that reliable CMC values for C_8E_5, C_8E_6, $C_{10}E_6$, and $C_{10}E_8$ are 3.15, 3.91, 0.38, and 0.51 g L^{-1}, respectively. These

values fit perfectly to the CMCs determined in this work. However, considerably less data are available regarding the influence of temperature on the CMC and thus the minimum in the CMC vs temperature curve is often unknown. Hence, we calculated the minimum in the CMC vs temperature curve from our experimental data using a second-order polynomial fit. We found the temperature of the minimum of the CMC of C_8E_5, C_8E_6, $C_{10}E_6$, and $C_{10}E_8$ to be at 50, 51, 47, and 55 °C, respectively. The minimum in the CMC for $C_{10}E_8$ was found by surface tension measurements at 61 °C,[21] while for $C_{12}E_j$ (j = 4, 6, 8), it was found to be around 50 °C.[20] These findings are in excellent agreement with our data. Extending the ethylene oxide chain is slightly shifting the minimum to higher temperatures. Contrarily, extending the alkyl chain is shifting the minimum to lower temperatures. The solubility of pure alkanes in water exhibits a minimum around room temperature. Therefore, a shift in the minimum temperature to lower temperatures is directly related to an increase in the hydrophobicity of the surfactant molecules. In line with this, extending the alkyl chain leads to a slight decrease of the minimum temperature. This was also found for other nonionic surfactants.[20−22,29]

Regarding the influence of the molecular structure of the surfactant (that is the hydrophilic ethylene oxide and the hydrophobic alkyl chain length) on the CMC, our results reveal two major findings: (1) Extending the alkyl chain by two carbon atoms leads to a decrease of the CMC by approximately 1 order of magnitude (see Table 1). This decrease in the CMC is directly related to the increase in hydrophobicity with extending alkyl chain length and is well known for both nonionic and ionic surfactants.[30−33] (2) Extending the hydrophilic ethylene oxide chain leads to an increase in the CMC. However, the influence of the ethylene oxide chain on the CMC is less pronounced compared to the alkyl chain. An increase in CMC with increasing ethylene oxide chain length results from an enhanced hydrophilicity and was also found for other C_iE_j surfactants.[20,34]

The results shown in Table 1 further reveal that extending the hydrophilic ethylene oxide chain increases the CMC more strongly at low temperatures (see C_8E_5 vs C_8E_6 and $C_{10}E_6$ vs $C_{10}E_8$). As mentioned above, at higher temperatures, the contribution of the alkyl chain to the CMC starts to predominate over the hydrophilic ethylene oxide chain. At 50 °C, the alkyl chain therefore mainly determines the CMC and the contribution of the ethylene oxide chain is of minor impact. Hence, the difference in the CMC with varying ethylene oxide and fixed alkyl chain length is higher at low temperatures and decreases with increasing temperature. Nonetheless, increasing the ethylene oxide chain leads to a slight increase in the CMC even at 50 °C.

3.2. Effect of Temperature, Concentration, and Molecular Structure of Surfactant on N_{agg} and R_h.
As described in the previous section, the interactions of same-type surfactant molecules with each other and with the surrounding bulk water are altered significantly upon changes in temperature. All surfactants investigated in this work exhibit a strong increase in N_{agg} with increasing temperature as also found for other C_iE_j surfactants.[25,35−37] The growth of N_{agg} can be explained similar to the decrease of the CMC with increasing temperature (see Section 3.1) by a decreasing intensity of the ethylene oxide chain interactions with the surrounding water molecules. At elevated temperatures, the effective head group area of the surfactant molecules is influenced by two major

processes: a dehydration of the ethylene oxide chain and a decrease in the density of the ethylene oxide chain.[19,38−40] While the former leads to a decrease of the effective head group area, the latter leads to an increase of the effective head group area. However, N_{agg} is increasing with increasing temperature. Therefore, the dehydration of the ethylene oxide chains must overcompensate for the decrease in the density of the ethylene oxide chains. Thus, more surfactant molecules can be incorporated in an aggregate at elevated temperatures.

The increase of N_{agg} with increasing temperature is generally higher for C_8E_5 and $C_{10}E_6$ compared to C_8E_6 and $C_{10}E_8$. Growth of C_iE_j surfactants aggregates increases rapidly as the binodal curve (or the cloud point for a given concentration) is approached.[35,41] Cloud points for C_8E_5, C_8E_6, $C_{10}E_6$, and $C_{10}E_8$ in water (at 10 g L^{-1}) are at 60, 74, 62, and 85 °C, respectively.[42,43] Thus, the rapid increase of N_{agg} with increasing temperature for C_8E_5 and $C_{10}E_6$ results from the proximity to their binodal curve in water, especially at 50 °C. Upon approaching the binodal curve, light scattering intensity is strongly influenced by concentration fluctuations.[17,44−46] For $C_{12}E_6$, it was found that these fluctuations start to dominate at approximately 10 K below the binodal curve, with this onset shifting toward the binodal curve at concentrations near the CMC.[24] However, we cannot exclude the contribution of these fluctuations to the overall light scattering intensity for C_8E_5 and $C_{10}E_6$ at 50 °C, and thus the N_{agg}'s at this temperature might be overestimated.

The molecular structure of the surfactant has a considerable influence on N_{agg}, as shown in Figure 1. Extending the hydrophilic ethylene oxide chain from E_5 to E_6 and from E_6 to E_8 leads to a decrease in N_{agg} due to an increasing effective head group area for a single surfactant molecule.[47] The decrease in N_{agg} for an extended ethylene oxide chain is stronger at elevated temperatures. While some authors attribute this to a transition temperature at which the aggregates start to grow from small monodisperse to large polydisperse aggregates,[48] others attribute this to a stronger contribution from the fluctuations near the binodal curve due to a shift of the binodal curve to higher temperatures upon extending the ethylene oxide chain.[44] On the other hand, extending the hydrophobic alkyl chain from C_8 to C_{10} at a constant E_6 increases the hydrophobic effect and thus the hydrophobic core volume.[30,49] Therefore, N_{agg} increases with increasing alkyl chain length for all temperatures investigated (see Figure 1).

Besides temperature, also increasing surfactant concentration leads to an increase in N_{agg} near the CMC for all investigated surfactants (see Figure 1). We studied N_{agg} in a concentration range starting from the CMC to approximately 2 times the CMC. N_{agg} values for the investigated surfactants available in the literature were all measured at considerably higher concentrations. Therefore, caution has to be taken when comparing N_{agg} values from this work and from the literature with respect to the measurement temperature and concentration. Table 2 compares N_{agg} values from this work and from the literature considering both measurement temperature and concentration.

For C_8E_5, our data show a strong increase of N_{agg} with concentration at all temperatures investigated (see Figure 1). This can also be seen when evaluating the N_{agg} data from the literature with respect to concentration and temperature. The same applies to $C_{10}E_6$ and $C_{10}E_8$, although our data reveals that

Table 2. Aggregation Numbers (N_{agg}) from This Work and the Literature for All Surfactants Investigated in This Work[a,b]

surfactant	T/°C	c/g L^{-1}	c/CMC	N_{agg}	ref
C_8E_5	25	70	20.77	90	50
	25	11.6	3.44	65	12
	25	6.3	1.87	59	this work
	30	17	5.25	80	51
	30	6.3	1.94	68	this work
C_8E_6	r. t.	n. g.		32	32
	25	11.7	2.99	45	12
	25	7.83	2	44	this work
	30	n. g.		41	52
$C_{10}E_6$	25	n. g.		73	52
	25	50	142.86	105	53
	25	1.91	5.46	74	12
	25	0.76	2.17	78	this work
	30	9.22	27.94	66	37
$C_{10}E_8$	25	n. g.		66	54
	25	50	89.29	70	53
	25	2.15	3.84	61	12
	25	1	1.79	57	this work

[a]r. t.: room temperature; n. g.: not given. [b]N_{agg} is given with respect to the temperature T and concentration c at which the measurements were conducted and c/CMC shows the factor by which the CMC is exceeded at the respective measurement concentration. CMCs from Table 1 were used to calculate c/CMC.

the increase of N_{agg} with concentration for these surfactants is lower compared to C_8E_5. However, the N_{agg} data in the literature for C_8E_6 shows no clear trend of N_{agg} with concentration. Possible reasons therefore are different measurement techniques that were used to obtain N_{agg} values. However, the N_{agg} values from this work show that N_{agg} is slightly increasing with concentration for C_8E_6. This emphasizes that a careful evaluation of the measurement concentration is necessary to obtain reliable N_{agg} values.

The R_h value of the aggregates is influenced by temperature and the molecular structure of the surfactant in the same way as N_{agg}. Increasing the temperature at a fixed concentration leads to an increase in R_h. Further, extending the ethylene oxide chain at a constant alkyl chain and extending the alkyl chain at a constant ethylene oxide chain leads to a decrease and an increase of R_h, respectively. The reasons for these are the same as for N_{agg} discussed above.

However, Figure 2 shows an abrupt increase in R_h as the CMC of the surfactant is exceeded. This increase in R_h with concentration is far more profound than the increase of N_{agg} with concentration. This can be explained considering the different ways of data processing for SLS and DLS. While SLS measures the excess Rayleigh ratio and thus only the scattering of the aggregates, DLS measures the overall (dynamic) scattering and thus also the contribution from the surfactant monomers. Therefore, DLS measures the average intensity-weighted translational diffusion coefficient of the aggregates including the contributions of the surfactant monomers (as no bimodal size distribution is obtained).[55] Hence, due to the monomer contribution, using diffusion coefficients from DLS near the CMC for calculating R_h of the aggregates leads to an underestimation of the actual size. However, as the concentration increases, the aggregate contribution soon starts to dominate the measured diffusion coefficient.[55] This can be

seen especially in Figure 2b for C_8E_6. For this surfactant, the obtained R_h values from the measured diffusion coefficients exhibit only a minor increase at higher concentrations. We measured an R_h value of 2.25 nm for C_8E_6 at 7.8 g L^{-1} and 25 °C, which is in perfect agreement with the R_h of 2.24 nm found at 11.7 g L^{-1} at the same temperature.[12] However, especially for $C_{10}E_6$ and $C_{10}E_8$, our data show that the diffusion coefficient and thus the obtained R_h values are still affected by the monomer contribution. Measurements at approximately 5 times the CMC resulted in R_h values of 2.80 nm and 2.90 nm for $C_{10}E_6$ and $C_{10}E_8$, respectively.[12] These values fit to the course of the R_h vs concentration curve measured in this work and emphasize that DLS data from surfactant solutions in the vicinity of the CMC must be evaluated carefully with respect to the contributions of surfactant monomers and aggregates.

4. CONCLUSIONS

In this work, the influence of temperature, concentration, and molecular structure (hydrophobic and hydrophilic chain lengths) on the self-assembly of four nonionic surfactants, C_8E_5, C_8E_6, $C_{10}E_6$, and $C_{10}E_8$, was investigated. Light scattering techniques (SLS and DLS) were used to determine the CMC as well as N_{agg} and R_h of the surfactant aggregates.

The CMCs of all investigated surfactants exhibit a minimum in their CMC vs temperature curve around 50 °C. This minimum results from a temperature-sensitive interplay of hydrophilic and hydrophobic interactions of the surfactant molecules among each other and with the surrounding water molecules. A significant growth of the surfactant aggregates with increasing temperature can be seen in both N_{agg} and R_h. Further, extending the hydrophobic alkyl chain by two carbon atoms leads to an increase of N_{agg} and R_h while simultaneously the CMC is reduced by approximately 1 order of magnitude. Contrarily, extending the ethylene oxide chain leads to a decrease of N_{agg} and R_h and a slight increase in the CMC.

The data shown in this paper further improve the understanding of the self-assembly of nonionic C_iE_j surfactants. The presented influence of temperature, concentration, and molecular structure on a microscopic scale facilitates the choice of a suitable surfactant for a given application, e.g., in a micellar solvent system, based on the surfactant aggregate structure.

5. MATERIALS AND METHODS

5.1. Preparation of Surfactant Solutions. Surfactants and Millipore water (Milli-Q Synthesis, Merck, Darmstadt, Germany) were weighted gravimetrically using a BP 301S analytical balance (Sartorius, Göttingen, Germany) with an accuracy of ±0.1 mg into a 15 mL Falcon tube (Corning, New York). The surfactants used in this work are listed in Table 3. The total volume of each surfactant solution was set to 10 mL.

Table 3. Surfactants Used in This Work with Molar Mass (M), Chemical Abstract Service (CAS) Number, Supplier, Mass Concentration as Given by the Supplier (w/v), and Purity

component	M/g mol^{-1}	CAS-No.	supplier	w/v	purity (%)
C_8E_5	350.5	19327-40-3	Anatrace	50	≥99
C_8E_6	394.5	4440-54-4	Anatrace	50	≥99
$C_{10}E_6$	422.6	5168-89-8	Anatrace	25	≥99
$C_{10}E_8$	510.7	24233-81-6	Sigma-Aldrich		≥98

All surfactant solutions were shaken thoroughly until the surfactant was fully dissolved. To remove emerging foam, the surfactant solution was subsequently centrifuged for 10 min at 3197g using an Eppendorf Centrifuge 5810 R (Hamburg, Germany). Afterward, the surfactant solution was filtered using a 0.1 μm hydrophilic poly(vinylidene fluoride) (PVDF) syringe filter (Berrytec, Harthausen, Germany). The filter was flushed with the surfactant solution before its use to ensure that the adsorption of surfactant molecules at the filter membrane was negligible.

5.2. Composition Gradient Multiangle Light Scattering. Surfactant solutions were analyzed using composition gradient multiangle light scattering (CG-MALS) measurements. The CG-MALS setup consists of a pumping and dosing unit (Calypso II), an SLS detector (DAWN HELEOS 8$^+$), and a refractive index (RI) detector (Optilab TrEX) from Wyatt Technology Corporation (Santa Barbara, CA). The DAWN HELEOS 8$^+$ measures the scattered light at eight different angles between 20 and 150°. To measure the SLS and DLS signals simultaneously, the SLS detector at 106° was replaced with a DLS detector (DynaPro Nanostar, Wyatt Technology Corporation, Santa Barbara, CA) using a glass fiber.

The surfactant solutions were mixed in a specific ratio with Millipore water using a static mixer with the Calypso II unit. The mixed solution was subsequently pumped through an online 0.02 μm filter membrane (Anodisc 13, GE Healthcare, Germany) and was then injected into the HELEOS 8$^+$ and Optilab TrEX. Afterward, the flow was stopped and the signals were measured for 5−10 min and light scattering intensities were averaged over the measurement time. The temperature of the DAWN HELEOS 8$^+$ and the Optilab TrEX was kept constant within ±0.01 K. This procedure was repeated automatically for different mixing ratios.

5.2.1. Static Light Scattering. Surfactant monomers self-assemble into aggregates above their CMC in water. This self-assembly causes a sudden increase in the intensity of scattered light.[16] SLS measures the time-averaged intensity of the scattered light expressed as the excess Rayleigh ratio for a vertically polarized light source according to eq 1.

$$R(\Theta) = \frac{(I(\Theta) - I_{solvent}(\Theta))r^2}{I_0 V} \quad (1)$$

Here, $I(\theta)$ and $I_{solvent}(\theta)$ are the total light scattering intensities of the solution and of the pure solvent both at a scattering angle θ, respectively. Intensities are normalized with respect to the intensity of the incident light I_0. Further, V is the scattering volume and r is the distance of the detector from the scattering volume. The CMC for a given surfactant can thus be obtained by measuring $R(\theta)$ for different surfactant concentrations. Within this work, $R(\theta)$ was measured for at least 10 different surfactant concentrations from concentrations lower than the CMC to approximately 2 times the CMC. The CMC was then obtained as the inflexion point in the slope of the $R(\theta)$ vs concentration plot.

Further, the M_W value of the surfactant aggregates was determined for different concentrations above the CMC using SLS. Since surfactant aggregates are growing with concentration, the classical double-extrapolation Zimm procedure cannot be applied to these systems.[25] To overcome this limitation, we studied dilute concentrations where interactions between the surfactant aggregates are negligible. The M_W value

of the aggregates was then obtained from SLS measurements using eq 2.

$$\frac{K^*(c - c_{CMC})}{R(\Theta) - R_{CMC}(\Theta)} = \frac{1}{M_W P(\Theta)} \quad (2)$$

Here, c is the total surfactant concentration, c_{CMC} is the surfactant concentration at the CMC, $R(\theta)$ and $R_{CMC}(\theta)$ are the total measured Rayleigh ratio and the Rayleigh ratio at the CMC, respectively, and $P(\theta)$ is the particle scattering function and gives the angular variation of the scattered light. However, for all systems investigated, no angular variation of the scattered light was observed and hence $P(\theta)$ was set to unity in this work. K^* is an optical constant and is defined according to eq 3

$$K^* = \frac{4\pi^2 n_0^2}{\lambda_0^2 N_A}\left(\frac{dn}{dc}\right)^2 \quad (3)$$

where n_0 is the refractive index of the solvent at the incident wavelength, λ_0 is the incident wavelength in vacuum, N_A is Avogadro's number, and dn/dc is the specific refractive index increment of the surfactant aggregates. We measured dn/dc for each surfactant at different temperatures using the RI detector. Only surfactant concentrations above the CMC were used to calculate dn/dc. N_{agg} was then obtained by dividing M_W by the molecular weight of the respective surfactant monomer.

5.2.2. Dynamic Light Scattering. DLS detects the intensity fluctuations of scattered light due to Brownian motion. Time-dependent intensity fluctuations are used to compute an intensity autocorrelation function that contains information about the diffusion of the surfactant molecules in solution. For a surfactant solution, DLS can thus measure the intensity-weighted translational diffusion coefficient D_t of the surfactant aggregates in solution. We used the cumulants analysis in the commercial software package ASTRA (WYATT Technology) to obtain D_t from the intensity autocorrelation function. In a next step, D_t was then used to calculate the hydrodynamic radius R_h of the surfactant aggregates according to the Stokes−Einstein equation (eq 4).

$$R_h = \frac{k_B T}{6\pi\eta D_t} \quad (4)$$

For that purpose, the temperature T, Boltzmann constant k_B, and dynamic viscosity η of the solution are required. Measurements of the solution viscosity showed no significant changes compared to the viscosity of water in the concentration range studied in this work (data not shown). Therefore, we used the viscosity of water at the respective temperature for η.

■ ASSOCIATED CONTENT

ⓈI Supporting Information

The Supporting Information is available free of charge at https://pubs.acs.org/doi/10.1021/acsomega.1c06766.

Measured Rayleigh ratios; refractive index increments; aggregation numbers; and hydrodynamic radii (PDF)

■ AUTHOR INFORMATION

Corresponding Authors

Christoph Brandenbusch − *Laboratory of Thermodynamics, Department of Biochemical and Chemical Engineering, TU Dortmund University, 44227 Dortmund, Germany;*

orcid.org/0000-0003-3338-9211;
Email: christoph.brandenbusch@tu-dortmund.de

Gabriele Sadowski − *Laboratory of Thermodynamics, Department of Biochemical and Chemical Engineering, TU Dortmund University, 44227 Dortmund, Germany;*
orcid.org/0000-0002-5038-9152;
Email: gabriele.sadowski@tu-dortmund.de

Authors

Peter Kroll − *Laboratory of Thermodynamics, Department of Biochemical and Chemical Engineering, TU Dortmund University, 44227 Dortmund, Germany;* orcid.org/0000-0001-9924-3261

Julius Benke − *Laboratory of Thermodynamics, Department of Biochemical and Chemical Engineering, TU Dortmund University, 44227 Dortmund, Germany*

Sabine Enders − *Institute for Technical Thermodynamics and Refrigeration, Karlsruhe Institute of Technology, 76131 Karlsruhe, Germany;* orcid.org/0000-0002-4287-9936

Complete contact information is available at:
https://pubs.acs.org/10.1021/acsomega.1c06766

Notes

The authors declare no competing financial interest.

ACKNOWLEDGMENTS

NOMENCLATURE

c	concentration g L^{-1}
dn/dc	specific refractive index increment mL g^{-1}
D_t	translational diffusion coefficient cm^2 s^{-1}
I	light scattering intensity V
k_B	Boltzmann's constant J K^{-1}
K^*	optical constant mol cm^2 g^{-2}
M_W	mass-averaged molecular weight g mol^{-1}
N_A	Avogadro's number mol^{-1}
N_{agg}	aggregation number
n	refractive index
$P(\Theta)$	particle scattering function
R_H	hydrodynamic radius nm
$R(\Theta)$	excess Rayleigh ratio cm^{-1}
r	distance of scattering volume from detector cm
T	temperature K
V	scattering volume cm^3
λ	wavelength of light nm
η	dynamic viscosity Pa s^{-1}

ABBREVIATIONS USED

CMC	critical micelle concentration
CG-MALS	composition gradient multiangle light scattering
D_t	mutual translational diffusion coefficient
DLS	dynamic light scattering
M_W	mass-averaged molecular weight
N_{agg}	aggregation number
R_h	hydrodynamic radius

SLS	static light scattering

REFERENCES

(1) Neslihan Gursoy, R.; Benita, S. Self-emulsifying drug delivery systems (SEDDS) for improved oral delivery of lipophilic drugs. *Biomed. Pharmacother.* **2004**, *58*, 173−182.

(2) Rangel-Yagui, C. O.; Pessoa, A., Jr; Tavares, L. C. Micellar solubilization of drugs. *J. Pharm. Pharm. Sci.* **2005**, *8*, 147−165.

(3) Nazar, M. F.; Shah, S. S.; Khosa, M. A. Microemulsions in Enhanced Oil Recovery: A Review. *Pet. Sci. Technol.* **2011**, *29*, 1353−1365.

(4) Kralova, I.; Sjöblom, J. Surfactants Used in Food Industry: A Review. *J. Disper. Sci. Technol.* **2009**, *30*, 1363−1383.

(5) Kim, E. J.; Kong, B. J.; Kwon, S. S.; Jang, H. N.; Park, S. N. Preparation and characterization of W/O microemulsion for removal of oily make-up cosmetics. *Int. J. Cosmet. Sci.* **2014**, *36*, 606−612.

(6) La Sorella, G.; Strukul, G.; Scarso, A. Recent advances in catalysis in micellar media. *Green Chem.* **2015**, *17*, 644−683.

(7) Schwarze, M.; Pogrzeba, T.; Volovych, I.; Schomäcker, R. Microemulsion systems for catalytic reactions and processes. *Catal. Sci. Technol.* **2015**, *5*, 24−33.

(8) Illner, M.; Müller, D.; Esche, E.; Pogrzeba, T.; Schmidt, M.; Schomäcker, R.; Wozny, G.; Repke, J.-U. Hydroformylation in Microemulsions: Proof of Concept in a Miniplant. *Ind. Eng. Chem. Res.* **2016**, *55*, 8616−8626.

(9) Pogrzeba, T.; Illner, M.; Schmidt, M.; Milojevic, N.; Esche, E.; Repke, J.-U.; Schomäcker, R. Kinetics of Hydroformylation of 1-Dodecene in Microemulsion Systems Using a Rhodium Sulfoxantphos Catalyst. *Ind. Eng. Chem. Res.* **2019**, *58*, 4443−4453.

(10) Sottmann, T.; Stubenrauch, C. Phase Behavior, Interfacial Tension and Microstructure of Microemulsions. In *Microemulsions: Background, new concepts, applications, perspectives*, 1st ed.; Wiley: Chichester, West Sussex, 2009; pp 1−47.

(11) Dong, R.; Hao, J. Complex fluids of poly(oxyethylene) monoalkyl ether nonionic surfactants. *Chem. Rev.* **2010**, *110*, 4978−5022.

(12) Swope, W. C.; Johnston, M. A.; Duff, A. I.; McDonagh, J. L.; Anderson, R. L.; Alva, G.; Tek, A. T.; Maschino, A. P. Challenge to Reconcile Experimental Micellar Properties of the CnEm Nonionic Surfactant Family. *J. Phys. Chem. B* **2019**, *123*, 1696−1707.

(13) Johnston, M. A.; Duff, A. I.; Anderson, R. L.; Swope, W. C. Model for the Simulation of the CnEm Nonionic Surfactant Family Derived from Recent Experimental Results. *J. Phys. Chem. B* **2020**, *124*, 9701−9721.

(14) Some, D.; Kenrick, S. Characterization of Protein-Protein Interactions via Static and Dynamic Light Scattering. In *Protein Interactions*; InTech: 2012; pp 401−426.

(15) Podzimek, Š. *Light scattering, size exclusion chromatography, and asymmetric flow field flow fractionation: Powerful tools for the characterization of polymers, proteins, and nanoparticles*; Wiley: Hoboken, NJ, 2011.

(16) Mazert, N. A. Laser Light Scattering in Micellar Systems. *Dynamic Light Scattering*; Springer: US, Boston, MA, 1985; pp 305−346.

(17) Williamson, J. C. Liquid−Liquid Demonstrations: Critical Opalescence. *J. Chem. Educ.* **2021**, *98*, 2364−2369.

(18) Kronberg, B.; Holmberg, K.; Lindman, B. *Surface Chemistry of Surfactants and Polymers*; Wiley: Chichester, 2014.

(19) Lindman, B.; Medronho, B.; Karlström, G. Clouding of nonionic surfactants. *Curr. Opin. Colloid Interface Sci.* **2016**, *22*, 23−29.

(20) Chen, L.-J.; Lin, S.-Y.; Huang, C.-C.; Chen, E.-M. Temperature dependence of critical micelle concentration of polyoxyethylenated non-ionic surfactants. *Colloids Surf., A* **1998**, *135*, 175−181.

(21) Chen, L.-J.; Lin, S.-Y.; Huang, C.-C. Effect of Hydrophobic Chain Length of Surfactants on Enthalpy−Entropy Compensation of Micellization. *J. Phys. Chem. B* **1998**, *102*, 4350−4356.

(22) Crook, E. H.; Trebbi, G. F.; Fordyce, D. B. Thermodynamic Properties of Solutions of Homogeneous p,t-Octylphenoxyethoxyethanols (OPE 1-10). *J. Phys. Chem.* **1964**, *68*, 3592−3599.

(23) Lindman, B.; Wennerstroem, H. Nonionic micelles grow with increasing temperature. *J. Phys. Chem.* **1991**, *95*, 6053−6054.

(24) Strey, R.; Pakusch, A. Critical Fluctuations, Micelle Kinetics and Phase Diagram of Water — Nonionic Surfactant, H2O — C12E6. *Surfactants in Solution*; Springer: US, Boston, MA, 1986; Vol. 4, pp 465−472.

(25) Bernheim-Groswasser, A.; Wachtel, E.; Talmon, Y. Micellar Growth, Network Formation, and Criticality in Aqueous Solutions of the Nonionic Surfactant C12E5. *Langmuir* **2000**, *16*, 4131−4140.

(26) Attwood, D.; Florence, A. T. *Surfactant Systems: Their Chemistry, Pharmacy and Biology*. Springer Netherlands, Dordrecht, 1983.

(27) Tsonopoulos, C. Thermodynamic analysis of the mutual solubilities of normal alkanes and water. *Fluid. Ph. Equilibria* **1999**, *156*, 21−33.

(28) Haarmann, N.; Enders, S.; Sadowski, G. Modeling binary mixtures of n-alkanes and water using PC-SAFT. *Fluid Phase Equilib.* **2018**, *470*, 203−211.

(29) Mohajeri, E.; Noudeh, G. D. Effect of Temperature on the Critical Micelle Concentration and Micellization Thermodynamic of Nonionic Surfactants: Polyoxyethylene Sorbitan Fatty Acid Esters. *Electron. J. Chem.* **2012**, *9*, 2268−2274.

(30) Tanford, C. *The Hydrophobic Effect: Formation of Micelles and Biological Membranes*, 2nd ed., Wiley: New York, 1980.

(31) Shinoda, K.; Nakagawa, T.; Bun-Ichi, T.; Isemura, T. *Colloidal Surfactants: Some Physicochemical Properties*; Academic Press: New York, 1963.

(32) Corkill, J. M.; Goodman, J. F.; Ottewill, R. H. Micellization of homogeneous non-ionic detergents. *Trans. Faraday Soc.* **1961**, *57*, 1627.

(33) Lindman, B.; Wennerström, H. Micelles. Amphiphile aggregation in aqueous solution. *Top. Curr. Chem.*; Springer-Verlag: 1980; pp 1−83.

(34) Rosen, M. J. *Surfactants and Interfacial Phenomena*, 3rd ed., Wiley-Interscience: Hoboken, NJ, 2004.

(35) Balmbra, R. R.; Clunie, J. S.; Corkill, J. M.; Goodman, J. F. Effect of temperature on the micelle size of a homogeneous non-ionic detergent. *Trans. Faraday Soc.* **1962**, *58*, 1661−1667.

(36) Einaga, Y. Wormlike Micelles of Polyoxyethylene Alkyl Ethers CiEj. *Polym. J.* **2009**, *41*, 157−173.

(37) Imanishi, K.; Einaga, Y. Effects of hydrophilic chain length on the characteristics of the micelles of pentaoxyethylene n-decyl C10E5 and hexaoxyethylene n-decyl C10E6 ethers. *J. Phys. Chem. B* **2005**, *109*, 7574−7581.

(38) Magazù, S. NMR, static and dynamic light and neutron scattering investigations on polymeric aqueous solutions. *J. Mol. Struct.* **2000**, *523*, 47−59.

(39) Maccarini, M.; Briganti, G. Density Measurements on C12Ej Nonionic Micellar Solutions as a Function of the Head Group Degree of Polymerization (j = 5−8). *J. Phys. Chem. A* **2000**, *104*, 11451−11458.

(40) Eliassi, A.; Modarress, H.; Mansoori, G. A. Densities of Poly(ethylene glycol) + Water Mixtures in the 298.15−328.15 K Temperature Range. *J. Chem. Eng. Data* **1998**, *43*, 719−721.

(41) Danov, K. D.; Kralchevsky, P. A.; Stoyanov, S. D.; Cook, J. L.; Stott, I. P.; Pelan, E. G. Growth of wormlike micelles in nonionic surfactant solutions: Quantitative theory vs. experiment. *Adv. Colloid Interface Sci.* **2018**, *256*, 1−22.

(42) Berthod, A. Polyoxyethylene alkyl ether nonionic surfactants: physicochemical properties and use for cholesterol determination in food. *Talanta* **2001**, *55*, 69−83.

(43) Huibers, P. D.; Shah, D. O.; Katritzky, A. R. Predicting Surfactant Cloud Point from Molecular Structure. *J. Colloid Interface Sci.* **1997**, *193*, 132−136.

(44) Corti, M.; Minero, C.; Degiorgio, V. Cloud point transition in nonionic micellar solutions. *J. Phys. Chem.* **1984**, *88*, 309−317.

(45) Zulauf, M.; Rosenbusch, J. P. Micelle clusters of octylhydroxyoligo(oxyethylenes). *J. Phys. Chem.* **1983**, *87*, 856−862.

(46) Schubert, K.-V.; Strey, R.; Kahlweit, M. A new purification technique for alkyl polyglycol ethers and miscibility gaps for water-CiEj. *J. Colloid Interface Sci.* **1991**, *141*, 21−29.

(47) Nagarajan, R.; Ruckenstein, E. Theory of surfactant self-assembly: a predictive molecular thermodynamic approach. *Langmuir* **1991**, *7*, 2934−2969.

(48) Puvvada, S.; Blankschtein, D. Molecular-thermodynamic approach to predict micellization, phase behavior and phase separation of micellar solutions. I. Application to nonionic surfactants. *J. Chem. Phys.* **1990**, *92*, 3710−3724.

(49) Padia, F. N.; Yaseen, M.; Gore, B.; Rogers, S.; Bell, G.; Lu, J. R. Influence of molecular structure on the size, shape, and nanostructure of nonionic C(n)E(m) surfactant micelles. *J. Phys. Chem. B* **2014**, *118*, 179−188.

(50) Zulauf, M.; Weckstrom, K.; Hayter, J. B.; Degiorgio, V.; Corti, M. Neutron scattering study of micelle structure in isotropic aqueous solutions of poly(oxyethylene) amphiphiles. *J. Phys. Chem.* **1985**, *89*, 3411−3417.

(51) Binana-Limbelé, W.; van Os, N. M.; Rupert, L.; Zana, R. Aggregation behavior and micellar dynamics in aqueous solutions of the nonionic surfactant pentaoxyethyleneglycol monooctyl ether: Effect of sodium halides. *J. Colloid Interface Sci.* **1991**, *144*, 458−467.

(52) Balmbra, R. R.; Clunie, J. S.; Corkill, J. M.; Goodman, J. F. Variations in the micelle size of non-ionic detergents. *Trans. Faraday Soc.* **1964**, *60*, 979−985.

(53) Alami, E.; Kamenka, N.; Raharimihamina, A.; Zana, R. Investigation on the Microstructures in Mixtures of Water with the Nonionic Surfactants C8E5, C10E6, and C10E8 in the Whole Range of Composition. *J. Colloid Interface Sci.* **1993**, *158*, 342−350.

(54) Ueno, M.; Kimoto, Y.; Ikeda, Y.; Momose, H.; Zana, R. Study on the aggregation number of mixed micelles in aqueous binary mixtures of the bile salts and nonionic surfactant. *J. Colloid Interface Sci.* **1987**, *117*, 179−186.

(55) Sutherland, E.; Mercer, S. M.; Everist, M.; Leaist, D. G. Diffusion in Solutions of Micelles. What Does Dynamic Light Scattering Measure?†. *J. Chem. Eng. Data* **2009**, *54*, 272−278.